

# Unraveling the magnetic ground-state in alkali-metal lanthanide oxide $\text{Na}_2\text{PrO}_3$ - Supplemental Materials

Ifeanyi John Onuorah,<sup>1</sup> Jonathan Frassinetti,<sup>2</sup> Qiaochu Wang,<sup>3</sup> Muhammad Maikudi Isah,<sup>2</sup> Pietro Bonfà,<sup>1</sup> Jeffrey G. Rau,<sup>4</sup> J. A. Rodriguez-Rivera,<sup>5,6</sup> A. I. Kolesnikov,<sup>7</sup> Vesna F. Mitrović,<sup>3</sup> Samuele Sanna,<sup>2</sup> and Kemp W. Plumb<sup>3</sup>

<sup>1</sup> Dipartimento di Scienze Matematiche, Fisiche e Informatiche,  
Università di Parma, I-43124 Parma, Italy

<sup>2</sup> Dipartimento di Fisica e Astronomia "A. Righi",  
Università di Bologna, I-40127 Bologna, Italy

<sup>3</sup> Department of Physics, Brown University, Providence, Rhode Island 02912, USA

<sup>4</sup> Department of Physics, University of Windsor, Windsor, Ontario, Canada N9B 3P4

<sup>5</sup>NIST Center for Neutron Research, National Institute of  
Standards and Technology, Gaithersburg, MD 20899, USA

<sup>6</sup>Department of Materials Science and Engineering,  
University of Maryland, College Park, MD 20742, USA

<sup>7</sup>Neutron Scattering Division, Oak Ridge National Laboratory, Oak Ridge, Tennessee 37831, USA

## I. MAGNETIC STRUCTURE AND $\mu$ SR DIPOLAR FIELD SIMULATIONS

Here we show in Fig S.1 the dipolar field distribution fit to the low temperature ZF- $\mu$ SR FFT power spectrum for all (28) the magnetic structures discussed in Appendix A of the main text. The plots of the four best fit reported in the main text are enclosed in blue colored border boxes and they capture the features of the highest amplitude peaks, lacking in the others.

## II. CEF CALCULATIONS

[!h] The single ion crystal electric field (CEF) calculations have been performed using PyCrystalField<sup>7</sup> software, in the intermediate coupling scheme with a spin-orbit coupling (SOC) constant of 54 meV in the LS basis, given  $L = 3$  and  $S = 1/2$ , so for a total of 14 LS values for each of the 7 (including the ground state) CEF eigenvalues. Details of these calculations are discussed in the main text while here, we show the  $\text{PrO}_6$  octahedral environment adapted for the calculations in Fig. S.2 and the resulting eigenvalues and eigenvectors tabulated in Tabs.II.

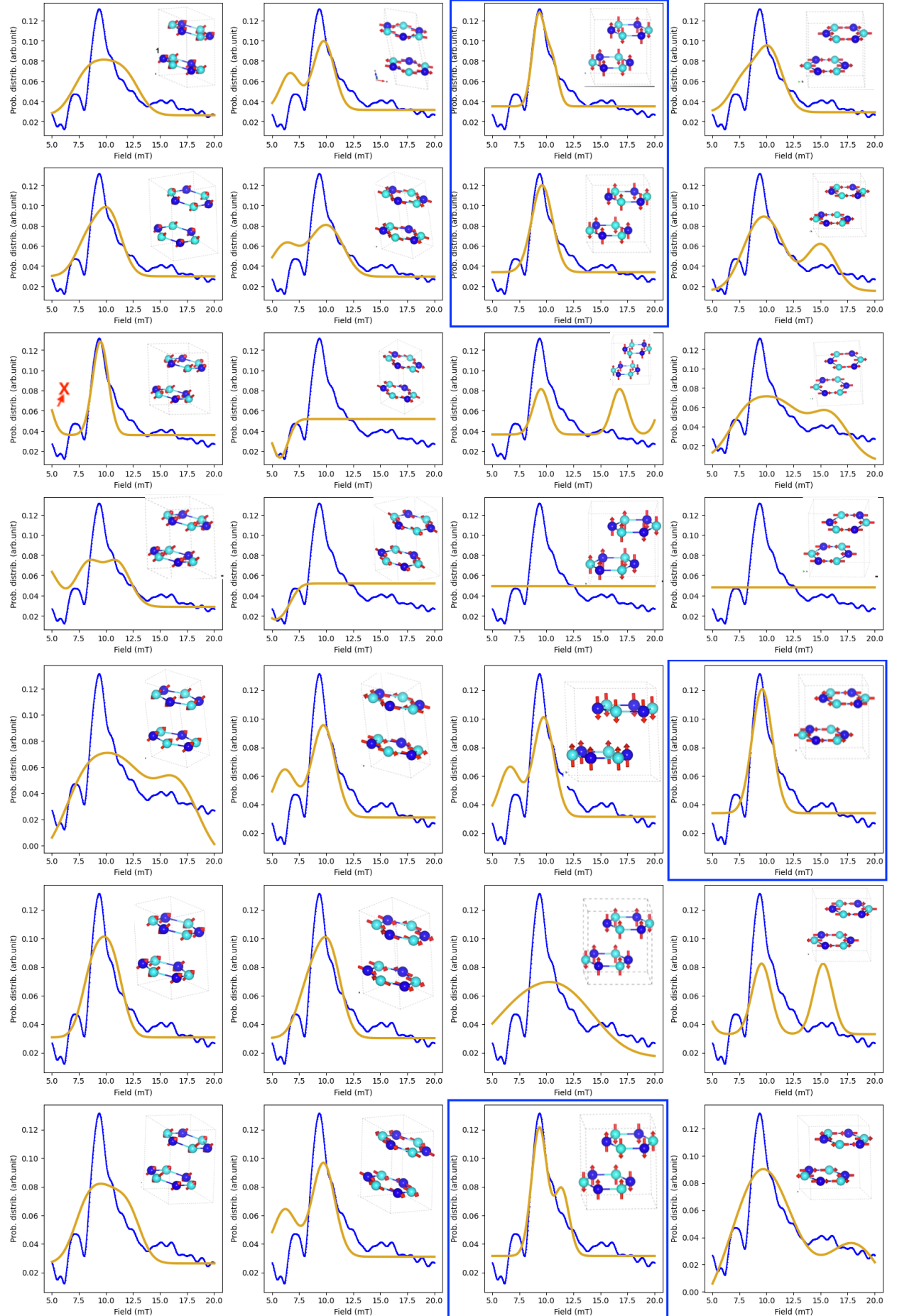


FIG. S.1: The calculated dipolar field fit distribution (yellow lines) to the zero field  $\mu$ SR FFT power spectrum (blue lines) for all the 28 candidate magnetic structures. Inset shows the magnetic structure. The plots of the four best fit reported in the main text are enclosed in blue colored border boxes.

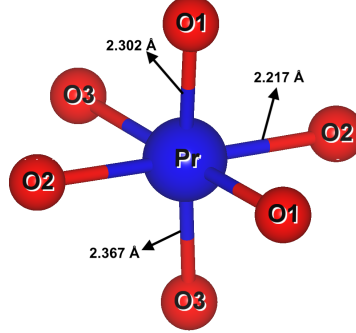


FIG. S.2: (a) The distorted  $\text{PrO}_6$  octahedra showing the distinct bond lengths, used for the point charge model calculations. CEF-PC model fit computed

TABLE S.I: Eigenvectors and Eigenvalues of the PC model fit to the INS data in the  $|L, S\rangle$  basis. The table is divided in two, with continuation along the row reported below.

E (meV)	$  -3, -\frac{1}{2} \rangle$	$  -3, \frac{1}{2} \rangle$	$  -2, -\frac{1}{2} \rangle$	$  -2, \frac{1}{2} \rangle$	$  -1, -\frac{1}{2} \rangle$	$  -1, \frac{1}{2} \rangle$	$  0, -\frac{1}{2} \rangle$
0.000	(-0.086+0j)	0j	0j	(0.155+0.163j)	(-0.346-0.478j)	0j	0j
0.000	0j	(0.143+0j)	(0.017-0.027j)	0j	0j	(0.444+0.562j)	(-0.17-0.173j)
225.480	(0.14+0j)	0j	0j	(-0.431+0.413j)	(-0.02-0.278j)	0j	0j
225.480	0j	(-0.487+0j)	(0.265+0.017j)	0j	0j	(0.118-0.345j)	(-0.251-0.206j)
242.810	(0.269+0j)	0j	0j	(0.098-0.302j)	(-0.155+0.393j)	0j	0j
242.810	0j	(0.465+0j)	(-0.403+0.063j)	0j	0j	(0.148-0.321j)	(-0.189+0.323j)
297.000	(-0.273+0j)	0j	0j	(-0.422+0.048j)	(-0.325+0.287j)	0j	0j
297.000	0j	(-0.498+0j)	(-0.11+0.028j)	0j	0j	(0.225+0.036j)	(0.087+0.486j)
389.870	0j	(0.217+0j)	(0.583+0.025j)	0j	0j	(0.295-0.184j)	(0.281-0.125j)
389.870	(0.333+0j)	0j	0j	(-0.139+0.35j)	(-0.088+0.369j)	0j	0j
529.260	0j	(0.08+0j)	(0.099-0.568j)	0j	0j	(0.152+0.119j)	(0.455+0.361j)
529.260	(0.273+0j)	0j	0j	(-0.314-0.255j)	(-0.103-0.193j)	0j	0j
568.510	0j	(0.474+0j)	(0.264+0.077j)	0j	0j	(-0.082-0.107j)	(-0.135+0.03j)
568.510	(-0.8+0j)	0j	0j	(-0.08-0.004j)	(0.021+0.124j)	0j	0j

E (meV)	$  0, \frac{1}{2} \rangle$	$  1, -\frac{1}{2} \rangle$	$  1, \frac{1}{2} \rangle$	$  2, -\frac{1}{2} \rangle$	$  2, \frac{1}{2} \rangle$	$  3, -\frac{1}{2} \rangle$	$  3, \frac{1}{2} \rangle$
0.000	(0.17-0.173j)	(-0.443+0.563j)	0j	0j	(-0.017-0.027j)	(-0.143+0j)	0j
0.000	0j	0j	(0.345-0.479j)	(-0.155+0.163j)	0j	0j	(0.086-0j)
225.480	(0.056+0.32j)	(0.358+0.067j)	0j	0j	(0.116-0.239j)	(-0.24+0.424j)	0j
225.480	0j	0j	(0.232+0.154j)	(-0.572+0.171j)	0j	0j	(0.069-0.122j)
242.810	(0.369+0.068j)	(-0.34-0.099j)	0j	0j	(0.311-0.264j)	(-0.304+0.352j)	0j
242.810	0j	0j	(0.399+0.14j)	(-0.292-0.123j)	0j	0j	(-0.176+0.204j)
297.000	(0.204+0.45j)	(-0.165+0.157j)	0j	0j	(0.107-0.04j)	(0.41-0.282j)	0j
297.000	0j	0j	(0.43+0.052j)	(0.374-0.2j)	0j	0j	(0.225-0.155j)
389.870	0j	0j	(0.312+0.216j)	(0.337+0.168j)	0j	0j	(-0.248+0.222j)
389.870	(-0.293+0.094j)	(-0.343+0.06j)	0j	0j	(-0.418+0.408j)	(-0.161+0.145j)	0j
529.260	0j	0j	(-0.16+0.149j)	(-0.38+0.139j)	0j	0j	(0.258+0.089j)
529.260	(0.548-0.193j)	(0.183-0.063j)	0j	0j	(-0.091+0.57j)	(0.076+0.026j)	0j
568.510	0j	0j	(0.08+0.097j)	(0.049-0.063j)	0j	0j	(0.524-0.605j)
568.510	(0.111-0.083j)	(-0.028-0.132j)	0j	0j	(-0.114+0.25j)	(-0.31+0.358j)	0j